



**HAL**  
open science

## Identification of instability mechanisms involved in the generation of railway curve squeal by point-contact models and modal bases

Van-Vuong Lai, Olivier Chiello, Jean-François Brunnel, Philippe Dufrenoy

### ► To cite this version:

Van-Vuong Lai, Olivier Chiello, Jean-François Brunnel, Philippe Dufrenoy. Identification of instability mechanisms involved in the generation of railway curve squeal by point-contact models and modal bases. Forum Acusticum, Dec 2020, LYON, France. pp. 2469-2475, 10.48465/fa.2020.0111 . hal-03233639

**HAL Id: hal-03233639**

**<https://hal.science/hal-03233639v1>**

Submitted on 26 May 2021

**HAL** is a multi-disciplinary open access archive for the deposit and dissemination of scientific research documents, whether they are published or not. The documents may come from teaching and research institutions in France or abroad, or from public or private research centers.

L'archive ouverte pluridisciplinaire **HAL**, est destinée au dépôt et à la diffusion de documents scientifiques de niveau recherche, publiés ou non, émanant des établissements d'enseignement et de recherche français ou étrangers, des laboratoires publics ou privés.

# IDENTIFICATION OF INSTABILITY MECHANISMS INVOLVED IN THE GENERATION OF RAILWAY CURVE SQUEAL BY POINT-CONTACT MODELS AND MODAL BASES

Van-Vuong Lai<sup>1</sup>      Olivier Chiello<sup>2</sup>  
Jean-François Brunel<sup>1</sup>      Philippe Dufrénoy<sup>1</sup>

<sup>1</sup> Univ. Lille, CNRS, Centrale Lille, UMR 9013 -

LaMcube - Laboratoire de Mécanique, Multiphysique, Multi-échelle, F-59000 Lille, France

<sup>2</sup> UMRAE, Univ Gustave Eiffel, IFSTTAR, CEREMA, Univ Lyon, F-69675, Lyon, France

vanvuong.lai1990@gmail.com, olivier.chiello@ifsttar.fr

## ABSTRACT

Squeal noise of rail-bound vehicles emitted in tight curves is characterized by high sound pressure levels at pure medium and high frequencies. The models used to simulate the vibrations that cause this noise differ in particular in terms of the instability mechanisms considered: negative damping introduced into the system due to the decrease in the friction coefficient with the sliding speed or instability with a constant friction coefficient. The objective of the paper is to contribute to the understanding of the instability mechanisms in the case of a constant friction coefficient. A stability analysis of the wheel/rail contact in curve is performed by using a point contact model combined with wheel and rail modal bases. Results show that even with an assumption of a constant Coulomb friction coefficient, instabilities can indeed occur due to the coupling between normal and tangential dynamics in the wheel/rail system. This coupling can involve two wheel modes, or only one when rail dynamics is included. The vertical dynamics of the rail then play an important role in the occurrence of the instability.

## 1. INTRODUCTION

Curve squeal is a noise often emitted when a railway vehicle (subway, tramway) come into a tight curve. This noise is characterized by a strong sound pressure which can reach 110 dB at 7.5 m from the track center in the range of 0 – 10000 Hz [1]. The measurements described by Rudd [2], Vincent *et al.* [3], Koch *et al.* [4] and Glocker *et al.* [5] show that the predominating part of squeal energy is concentrated in one or several pure tone frequencies close to natural frequencies of the wheel [3]. It is also observed that curve squeal depends strongly on the local kinematic parameters at wheel/rail contact, the friction at contact interface and the wheel vibro-acoustic characteristics [4].

It is well accepted in the literature that the high lateral slip of the wheel on the rail-head is the main cause of curve squeal [2,3,6]. The friction forces generated by this sliding motion may lead to structural instability and self-sustained vibration of the wheel/rail system. This self-sustained vi-

bration is also considered as a kind of friction-induced vibrations.

In the literature, the results of existing curve squeal models correspond well to experimental observations such as instabilities of axial modes with zero nodal circle and creep/slip limit cycles. However, the instability mechanisms are still controversial. This makes it difficult to find solutions for reduction of this noise. In [2, 7–15], authors considered that a friction coefficient decreasing with creep velocities triggers instabilities even if the rail dynamics is not included. A falling slope in the velocity-dependent friction law can be mathematically expressed as a negative damping leading to an unstable behavior [16–18]. However, experimentally, it is difficult to measure the dynamic creep quantities (especially contact forces) and only apparent friction coefficient is measured. Moreover, the slope of the friction coefficient is not really proved in experimental terms [4]. In the case of constant friction coefficient and when the rail dynamics is included, instabilities are also found [14, 19–21]. To explain this kind of instability, two instability mechanisms are highlighted by Ding *et al.* [22] and Lai *et al.* [23]. The first one is mode coupling [24, 25] which can be explained mathematically by the non-symmetric stiffness matrix due to friction. The second one is instability of a single wheel mode caused by equivalent mass and damper behaviors of the rail [22] or only an equivalent damper behavior of the rail [23].

The aim of this paper is to identify the mechanisms responsible for curve squeal in order to propose potential solutions for the reduction of this noise. In Section 2, the method developed in [23] is presented. A stability analysis is performed around the equilibrium state by using a point-contact model (Hertz's theory for the normal contact problem and an assumption of full lateral sliding state at the contact zone). The wheel/rail responses are computed by using wheel/rail modal bases. In Section 2, the effect of parameters are investigated in order to propose reduction solutions.

## 2. STABILITY ANALYSIS FOR A WHEEL/RAIL CONTACT SYSTEM IN CURVE

### 2.1 Statement of the problem

The wheel/rail interaction model is described in Fig. 1. The normal contact is assumed to be Hertzian so that the normal contact force can be analytically determined. The lateral friction force satisfies the Coulomb law with a constant friction coefficient  $\mu$ . A full lateral sliding of the wheel on the rail is assumed.  $s_y$  denotes lateral creepage.  $s_y > 0$  corresponding to the sliding of the inner wheel and  $s_y < 0$  corresponding to the sliding of the outer wheel.

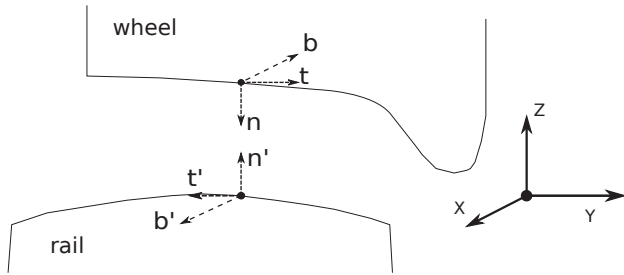


**Figure 1:** Reference frame of the wheel/rail interaction. The rolling direction along the rail is the  $x$ -direction. The lateral direction is the  $y$ -direction. The vertical direction is the  $z$ -direction.  $(n, t, b)$  and  $(n', t', b')$  are respectively the local frames of the wheel and the rail such that:  $n' = -n = Z$ ,  $t' = -t = -Y$ ,  $b' = -b = X$

### 2.2 Stability analysis

Stability analysis is based on the linearization of the equation of motion governing the wheel/rail contact system. By using the normal modal bases  $\Phi$  computed from the wheel/rail models combining with the linearization of frictional contact forces, an eigenvalue problem can be obtained given by:

$$\mathbf{M}_{\text{red}}\ddot{\mathbf{q}} + \mathbf{C}_{\text{red}}\dot{\mathbf{q}} + (\mathbf{K}_{\text{red}} + \mathbf{K}_{\mu})\mathbf{q} = 0 \quad (1)$$

where  $\mathbf{q}$  is the dynamic perturbation of generalized coordinates vector around the total sliding equilibrium.  $\mathbf{M}_{\text{red}}$ ,  $\mathbf{K}_{\text{red}}$ ,  $\mathbf{C}_{\text{red}}$  are the reduced mass, stiffness and damping matrix corresponding to the base  $\Phi$ .  $\mathbf{K}_{\mu}$  is a matrix which takes into account the frictional contact forces and is not symmetric due to the coupling of the normal and tangential dynamics through friction coefficient  $\mu$ . The detail of these matrices can be found in [23].

A complex modal analysis of Eq. (1) can be performed to evaluate the complex modes. The solution is sought in the form:  $\mathbf{q} = \mathbf{q}_0 e^{\lambda t}$  where  $\mathbf{q}_0$  is the complex amplitude of  $\mathbf{q}$  and  $\lambda$  is a complex number. Eq. (1) becomes:

$$(\lambda^2 \mathbf{M}_{\text{red}} + \mathbf{C}_{\text{red}}\lambda + (\mathbf{K}_{\text{red}} + \mathbf{K}_{\mu}))\mathbf{q}_0 = 0 \quad (2)$$

Unstable modes are identified with a positive real part of the corresponding complex eigenfrequencies  $\lambda$ . The divergence rate of a mode is defined as the ratio between the real and imaginary part of the complex mode:

$$DvR = \text{Real}(\lambda)/\text{Imag}(\lambda) \quad (3)$$

where  $\text{Real}(\lambda)$  and  $\text{Imag}(\lambda)$  are the real and imaginary parts of the associated complex mode.

### 2.3 Wheel and rail FE models

In this section, the finite element (FE) wheel and rail models used for the calculation of modal bases are presented. The material data of the wheel and the rail are listed in Tab. 1. As mentioned in [23], these models allow for an extraction of the stiffness and mass matrices which are then used to calculate normal modal bases and the reduced stiffness, mass and viscous damping matrices in Eq. (1). The detail and the validation of these models can be found in [23].

Data	Wheel	Rail
Young's modulus (GPa)	206.9	205
Poisson's ratio	0.288	0.3
Density ( $kg/m^3$ )	7800	7800

**Table 1:** Material data of the wheel and the rail

The wheel model is a wheel of type "Vyksa BA005" (Fig. 2). A rigid constraint is applied at the inner face of the hub, where the wheel is connected to the axle. This boundary condition avoids getting rigid mode in the modal basis. The natural frequencies and corresponding free-interface modes have then been calculated up to 5000 Hz. As in [20, 21, 26], these modes may be distinguished according to the dominant movement (radial modes, axial modes and circumferential modes), the number of nodal diameters  $n_d$  and the number of nodal circles  $n_c$ . Classical modal damping factors  $\xi^w$  are chosen depending on the nodal diameters  $n_d$  [27].

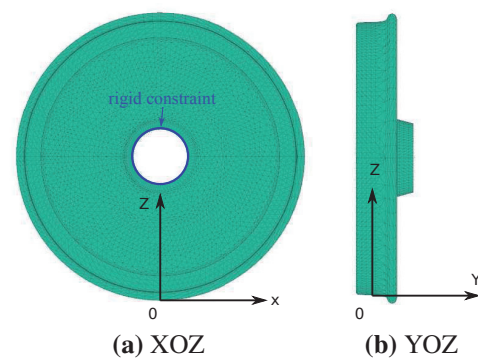


**Figure 2:** Wheel FE mesh with a nominal rolling diameter of 920 mm and a mass of 314 kg

A FE track model allowing the cross-sectional deformations and the behavior associated with the "pinned-pinned" effect is adopted. The track model consists in one periodically supported rail of UIC60 type (Fig. 3). This rail is 48 m long. The space between the sleepers (sleeper span) is 60 cm. The track support contains only elastic

pads that connect the rail and each sleeper. They are modeled by springs of longitudinal, lateral and vertical stiffnesses  $K_x = K_y = 36, K_z = 180$  MN/m for each sleeper. The pad structural damping is set to  $\eta_s = 1$ . The contact position is in the center of the rail in the  $x$ -axis. The rail structural damping is  $\eta = 0.02$ . Anechoic terminations are obtained by gradually increasing the rail damping from 2% to 100% [28] in order to avoid the reflexion of waves in a FE model [28]. The natural frequencies and corresponding free-interface modes  $\Phi^r$  have been calculated up to 5000 Hz.

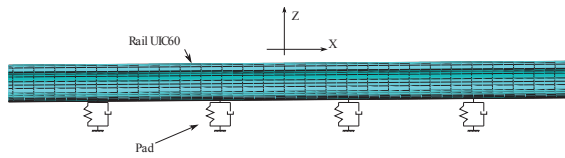


Figure 3: Track model

### 2.4 Numerical results

Four unstable modes (with positive real part) are obtained using the reference data in Table 2. The frequency of these unstable complex modes are 334, 918, 1671 and 3418 Hz respectively which get close to the frequencies of the 4 axial wheel modes with (2,3,4,6) nodal diameters and 0 nodal circle (Figure 4). The result is consistent with experimental observations [3, 4, 7].

Rolling velocity $V$ (m/s)	10
Imposed lateral velocity of the wheel $V_y$ (m/s)	0.1
Friction coefficient $\mu$	0.3
Static vertical load $N$	7 kN

Table 2: Kinematic parameters of the wheel/rail rolling contact model

To analyze the instability mechanism, it is useful to compute the bifurcation curves representing the evolution of the unstable modes as a function of friction coefficient  $\mu$  while the other parameters are kept constant. The bifurcation curves of the unstable complex modes are presented in Fig. 5. The bifurcation curves in Fig. 5d shows a coupling between two complex modes. There is no perfect coalescence between the two frequencies due to the system damping. These curves are the same as the form of the bifurcation curves in case of mode coupling [25]. It is concluded that mode coupling is responsible for this instability. On the other hand, for the first three unstable modes (a,0,2), (a,0,3) and (a,0,4), the form of the bifurcation curves is different and no mode coupling is found. According to Ding *et al.* [29], this instability of a single wheel mode is due to the mass and damper behaviors of the track.

In order to explain the second type of instabilities due to coupling between the normal and tangential components of the single wheel mode when the rail dynamics, a reduced model (Fig. 6) allowing to explain the kind of instabilities

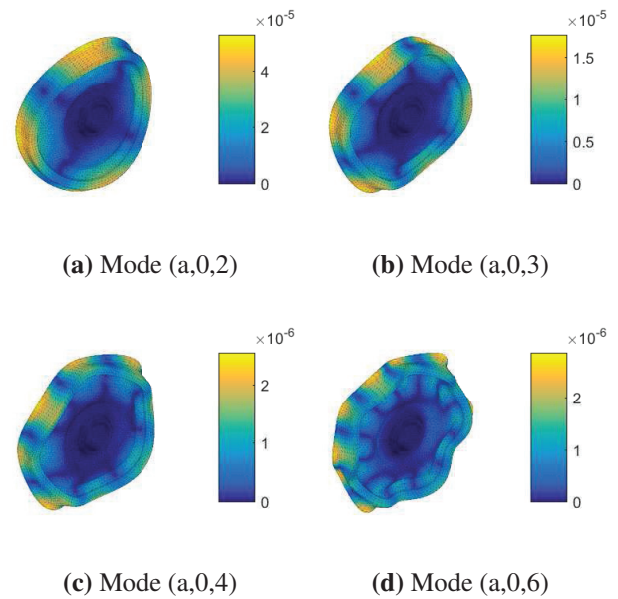


Figure 4: Unstable modes shapes for  $\mu = 0.3$

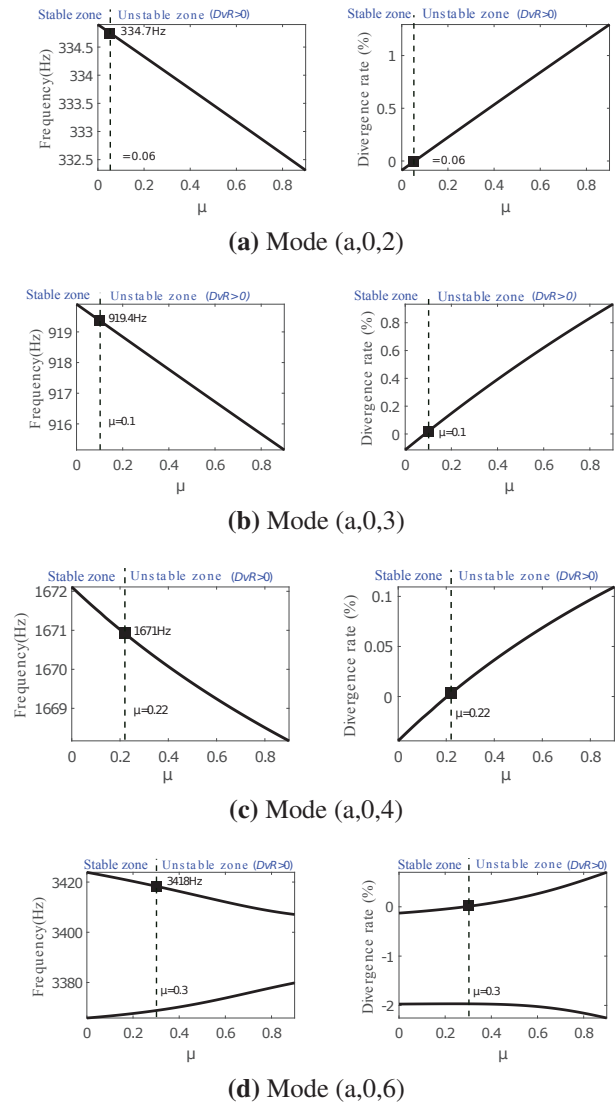
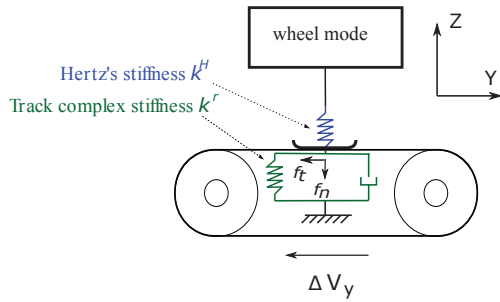


Figure 5: Bifurcation curves of the unstable complex modes with the flexible track

was developed. The mechanical system is represented by one wheel mode of natural pulsation  $\Omega$ , damping factor  $\xi^w$  and contact modal amplitudes  $\Phi_z^w$  and  $\Phi_y^w$ , coupling with an Hertz's stiffness  $k^H$  representing the contact [27] and an equivalent complex stiffness  $k^r$  representing the track vertical dynamics. Only the track vertical dynamics are considered because it is found that the track lateral dynamics are not involved in these instabilities [23]. The imaginary part of complex stiffness  $k^r$  mainly due to the phase shift of the propagating wave but also to structural damping effects [27] is considered as a damper equivalent to the behavior of an infinite track.



**Figure 6:** Simple 1-DOF model for instabilities due to the rail vertical phase response

The solution of this mechanical system (Fig. 6) is sought in a form of  $X = X_o(\omega)e^{i\omega t}$  where  $\omega$  is pulsation and  $X_o(\omega)$  is the amplitude of this solution. As in section 2, the modal basis is used here which contains only a wheel mode. An eigenvalue equation is obtained as:

$$(-\omega^2 + 2i\omega\xi^w\Omega + \Omega^2 + K_c)q = 0 \quad (4)$$

where

$$K_c = (\Phi_z^w - \mu \text{sign}(s_{y0})\Phi_y^w) \frac{k^H k^r}{k^H + k^r} \Phi_z^w \quad (5)$$

is the complex stiffness due to the contact, the friction, the wheel modal amplitudes and the rail vertical dynamics. The imaginary part of this complex stiffness  $K_c$  results from the imaginary part of the rail stiffness.

Assuming that near the natural frequency of the considered wheel mode,  $K_c(\omega) \approx K_c(\Omega)$ , an equivalent viscous modal damping factor can be introduced in the system due to this complex stiffness  $K_c$ :

$$\eta_c = \frac{\text{Imag}(K_c)}{2\Omega^2} \quad (6)$$

where  $\text{Imag}(\bullet)$  denotes respectively the imaginary part of  $(\bullet)$ . Thus, the total damping factor  $\xi_c$  is thus given by:

$$\xi_c = \xi^w + \eta_c \quad (7)$$

where  $\xi^w$  is the natural modal damping factor of the wheel mode. The sign of damping factor  $\xi_c$  (Eq. (7)) is the key factor for the stability of the system. If this damping factor is negative, the divergence rate is positive and the wheel/rail system becomes unstable.

Fig. 7 shows the linear evolution of the divergence rate of the unstable modes since the relation between the imaginary part of  $K_c$  and  $\mu$  is linear (Eq. (5)). The results obtained by this reduced model are similar to the results obtained by the full FE track model. Thus, it can be concluded that the imaginary part of the track vertical complex stiffness is responsible for the instabilities of a single wheel mode.

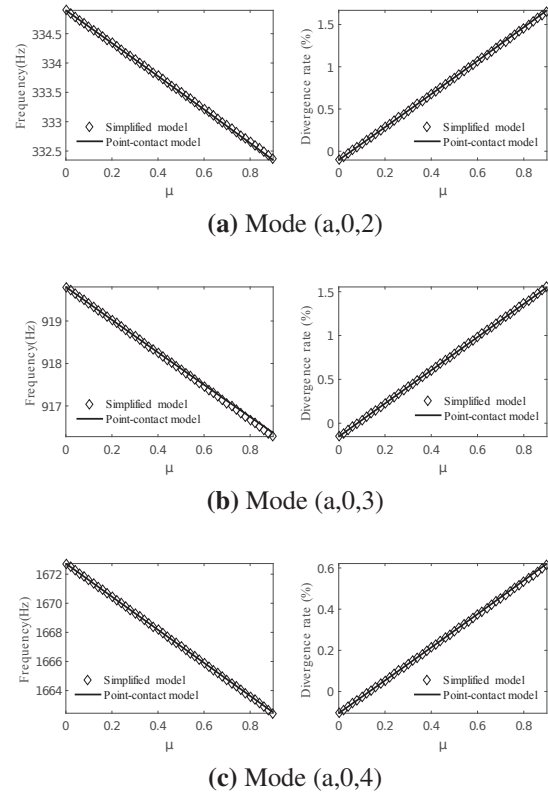


**Figure 7:** Bifurcation curves of the unstable complex modes for the 1-DOF model

In this section, the mechanisms which explains instabilities are identified in the case of constant friction coefficient. It is found that instabilities can be triggered by mode coupling and the equivalent damper behavior of the track. Thus, not only the wheel dynamics but also the track dynamics are involved in these instabilities.

### 3. PARAMETRIC STUDY

In order to find potential solutions for the reduction of this noise, a parametric study is performed to investigate the effects of main parameters.

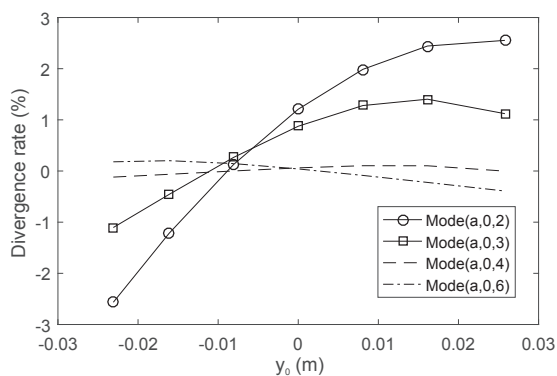
#### 3.1 Effect of the contact position on the wheel and creepage sign

In this study, as in De Beer *et al.* model [15], it is assumed that the contact position on the rail does not change. Only the  $y$ - coordinate of the contact point on the wheel  $y_0$  varies. All other parameters are maintained constant.

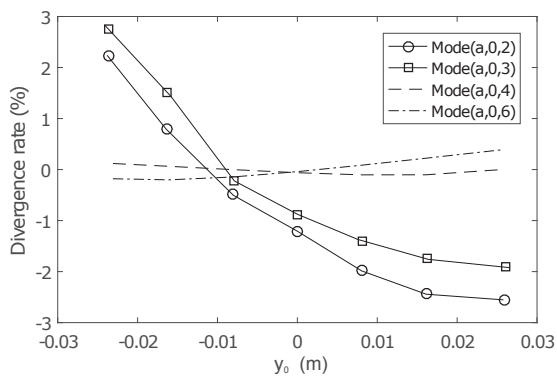
Fig. 8 shows the strong influence of the contact position on the wheel combined with the sign of  $s_y$ . In the

case of sliding inner wheel ( $s_y > 0$ ), the divergence rates of the unstable complex modes (a,0,2), (a,0,3) and (a,0,4) increase when the contact position gets close to the flange ( $y_0$  increases). This result is similar to the result of De Beer's model [15] but is opposed to the result of Pieringer's model [19]. On the other hand, the divergence rate of the unstable complex mode (a,0,6) decreases while the contact position gets close to the flange.

In the case of sliding outer wheel ( $s_y < 0$ ), the results are contrary to the results corresponding to the sliding inner wheel. The unstable complex modes (a,0,2), (a,0,3) and (a,0,4) appear when the contact position is far from flange. By taking into account the behavior of railway bogies in curve, the contact position of the outer wheel is close to the flange. Thus, for the outer wheel, the occurrence probability of the unstable complex modes (a,0,2), (a,0,3) and (a,0,4) is lower than for the inner wheel.



(a)  $s_y > 0$



(b)  $s_y < 0$

**Figure 8:** Divergence rate of unstable complex modes as a function of the contact position on the wheel

### 3.2 Effect of the wheel modal damping

The effect of the wheel modal damping factors are showed in (Fig. 9). We can observe that when the modal damping factor of the axial wheel modes (a,0,2), (a,0,3), (a,0,4) and (a,0,6) reach 0.2%, 0.15%, 0.02% and 0.1% respectively, the associated unstable complex modes become stable. Thus, squeal occurrence tends to reduce if the damp-

ing of the implicated axial wheel modal increases. The modal damping factors do not agree with the 1.3 – 3% range of critical damping factor needed to avoid squealing on the mode (a,0,2) founded experimentally by Koch *et al.* [4] on a 1/4 scale test rig. It is difficult to conclude here because the two systems are not the same. The rail in Koch *et al.*'s test [4] is not a real rail and is represented by a wheel with a large diameter. In any case, the obtained critical damping factors are quite low compared with those generally observed in the literature. This point deserves to be further explored. A (too) low friction coefficient (equal to 0.3 here) might explain this difference.

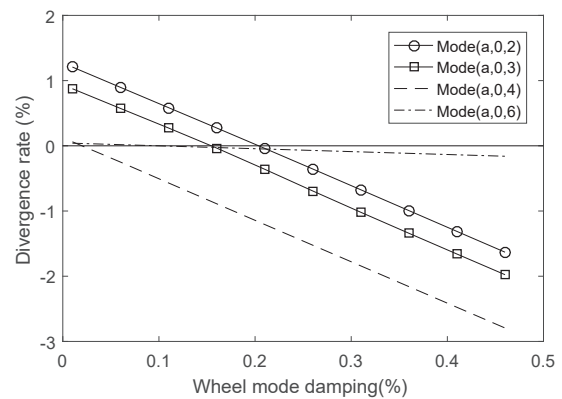


**Figure 9:** Divergence rate of unstable complex modes as a function of the associated axial wheel modes

### 3.3 Effect of vertical pad stiffness

While the parameters of the reference case are maintained constant, if the vertical pad stiffness  $k_{pad}$  increases, the divergence rate of the unstable modes (a,0,2) and (a,0,3) greatly decreases as shown in Fig. 10. The divergence rate of the unstable modes (a,0,4) firstly decreases and then increases. The divergence rate of the unstable mode (a,0,6) does not change. Chen [30] also found that an increase of the track vertical pad stiffness can reduce the instability of unstable mode. It can be explained by the fact that an increase of the vertical pad stiffness implies an decrease of the rail vertical flexibility, which decreases the level of coupling. However, the effect of the vertical pad stiffness is not straightforward and seem to depend on other parameters.

## 4. CONCLUSION

A stability analysis of wheel/rail rolling contact in the case of lateral full sliding was performed in order to identify the instability mechanisms. A point contact model with linearized Hertzian normal law and Coulomb's friction law is used. The wheel and rail dynamics are computed by using modal bases. It was found that even with a constant Coulomb friction, instabilities can occur because of two mechanisms: mode coupling and the equivalent damper behavior of the rail induced by the phase shift of the propagating wave but also by pad and rail damping. Mode

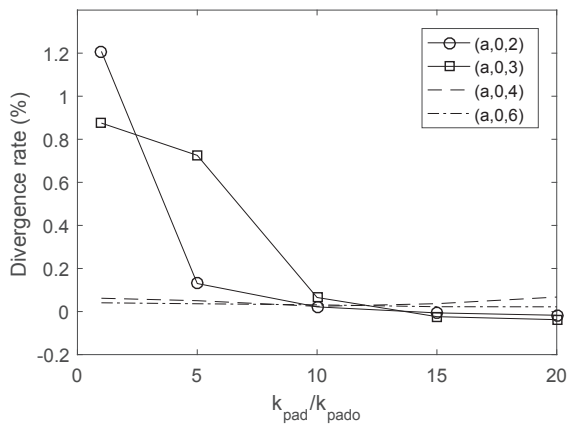


**Figure 10:** Influence of the pad vertical stiffness on the unstable complex modes ( $k_{pado}$ : vertical pad stiffness in the reference case)

coupling can involve two wheel modes (mode coupling) whereas the second mechanism can involve only one wheel mode (among axial modes with 2 to 4 nodal diameters and 0 nodal circle).

Since the rail dynamics play a crucial role in instability of wheel/rail system in curve, mitigation solutions must not only focus on the wheel but also on the track. In addition to the increase of the damping of the wheel (Eq. (7)), the parametric study showed that the occurrence of instability depends mainly on friction coefficient, contact position and rail vertical pad stiffness. From this study, two solutions to reduce curve squeal can be proposed is the increase of wheel damping and rail vertical stiffness.

## 5. ACKNOWLEDGEMENT

This work was carried out within the CERVIFER project backed by the ADEME organization and the Haut-de-France region and within the framework of the LABEX CeLyA (ANR-10-LABX-0060) of University of Lyon, within the program "Investissements d'Avenir" (ANR-11-IDEX-0007) operated by the French National Research Agency (ANR). The authors gratefully acknowledge the support of these institutions.

## 6. REFERENCES

- [1] D. Eadie and M. Santoro, "Top-of-rail friction control for curve noise mitigation and corrugation rate reduction," *Journal of Sound and Vibration*, vol. 293, pp. 747–757, 2006.
- [2] M. Rudd, "Wheel/rail noise-part ii: Wheel squeal," *Journal of Sound and Vibration*, vol. 46, pp. 381–394, 1976.
- [3] N. Vincent, J. Koch, H. Chollet, and J. Guerder, "Curve squeal of urban rolling stockpart 1: State of the art and field measurements," *Journal of sound and vibration*, vol. 293, pp. 691–700, 2006.
- [4] J. Koch, N. Vincent, H. Chollet, and O. Chiello, "Curve squeal of urban rolling stockpart 2: Parametric study on a 1/4 scale test rig," *Journal of sound and vibration*, vol. 293, pp. 701–709, 2006.
- [5] C. Glocker, E. Cataldi-Spinola, and R. Leine, "Curve squealing of trains: Measurement, modelling and simulation," *Journal of Sound and Vibration*, vol. 324, pp. 365–386, 2009.
- [6] P. Remington, "Wheel/rail squeal and impact noise: What do we know? what don't we know? where do we go from here?," *Journal of Sound and Vibration*, vol. 116, pp. 339–353, 1987.
- [7] C. Van Ruiten, "Mechanism of squeal noise generated by trams," *Journal of Sound and Vibration*, vol. 120, pp. 245–253, 1988.
- [8] E. Schneider, K. Popp, and H. Irretier, "Noise generation in railway wheels due to rail-wheel contact forces," *Journal of Sound and Vibration*, vol. 120, pp. 227–244, 1988.
- [9] U. Fingberg, "A model of wheel-rail squealing noise," *Journal of Sound and Vibration*, vol. 143, pp. 365–377, 1990.
- [10] F. J. Périard, *Wheel-rail noise generation: curve squealing by trams*. TU Delft, Delft University of Technology, 1998.
- [11] M. A. Heckl and I. Abrahams, "Curve squeal of train wheels, part 1: mathematical model for its generation," *Journal of Sound and Vibration*, vol. 229, pp. 669–693, 2000.
- [12] M. A. Heckl, "Curve squeal of train wheels, part 2: Which wheel modes are prone to squeal?," *Journal of Sound and Vibration*, vol. 229, pp. 695–707, 2000.
- [13] O. Chiello, J.-B. Ayasse, N. Vincent, and J.-R. Koch, "Curve squeal of urban rolling stockpart 3: Theoretical model," *Journal of sound and vibration*, vol. 293, pp. 710–727, 2006.
- [14] B. Ding, G. Squicciarini, and D. Thompson, "Effects of rail dynamics and friction characteristics on curve squeal," in *Journal of Physics: Conference Series*, vol. 744, p. 012146, IOP Publishing, 2016.
- [15] F. De Beer, M. Janssens, and P. Kooijman, "Squeal noise of rail-bound vehicles influenced by lateral contact position," *Journal of Sound and Vibration*, vol. 267, pp. 497–507, 2003.
- [16] K. Popp and P. Stelter, "Stick-slip vibrations and chaos," *Philosophical Transactions: Physical Sciences and Engineering*, pp. 89–105, 1990.
- [17] M. Bengisu and A. Akay, "Stability of friction-induced vibrations in multi-degree-of-freedom systems," *Journal of Sound and Vibration*, vol. 171, pp. 557–570, 1994.

- [18] R. Ibrahim, “Friction-induced vibration, chatter, squeal, and chaos part i: Mechanics of contact and friction,” *Applied Mechanics Reviews*, vol. 47, pp. 209–226, 1994.
- [19] A. Pieringer, “A numerical investigation of curve squeal in the case of constant wheel/rail friction,” *Journal of Sound and Vibration*, vol. 333, pp. 4295–4313, 2014.
- [20] I. Zenzerovic, W. Kropp, and A. Pieringer, “An engineering time-domain model for curve squeal: Tangential point-contact model and green’s functions approach,” *Journal of Sound and Vibration*, vol. 376, pp. 149–165, 2016.
- [21] I. Zenzerovic, W. Kropp, and A. Pieringer, “Influence of spin creepage and contact angle on curve squeal: A numerical approach,” *Journal of Sound and Vibration*, vol. 419, pp. 268–280, 2018.
- [22] B. Ding, G. Squicciarini, and D. Thompson, “Effect of rail dynamics on curve squeal under constant friction conditions,” *Journal of Sound and Vibration*, vol. 442, pp. 183–199, 2019.
- [23] V.-V. Lai, O. Chiello, J.-F. Brunel, and P. Dufrénoy, “The critical effect of rail vertical phase response in railway curve squeal generation,” *International Journal of Mechanical Sciences*, vol. 167, p. 105281, 2020.
- [24] J. Oden and J. Martins, “Models and computational methods for dynamic friction phenomena,” *Computer methods in applied mechanics and engineering*, vol. 52, pp. 527–634, 1985.
- [25] N. Hoffmann, M. Fischer, R. Allgaier, and L. Gaul, “A minimal model for studying properties of the mode-coupling type instability in friction induced oscillations,” *Mechanics Research Communications*, vol. 29, pp. 197–205, 2002.
- [26] A. Pieringer, “Time-domain modelling of high-frequency wheel/rail interaction [dissertation],” *Göteborg: Chalmers University of Technology*, 2011.
- [27] D. Thompson, *Railway noise and vibration: mechanisms, modelling and means of control*. Elsevier, 2008.
- [28] B. Betgen, G. Squicciarini, and D. J. Thompson, “On the prediction of rail cross mobility and track decay rates using finite element models,” in *Proceedings of the In Proceedings of the 10th European Congress and Exposition on Noise Control Engineering*, p. 2019, 2015.
- [29] B. Ding, G. Squicciarini, D. Thompson, and R. Corradi, “An assessment of mode-coupling and falling-friction mechanisms in railway curve squeal through a simplified approach,” *Journal of Sound and Vibration*, vol. 423, pp. 126–140, 2018.
- [30] G. Chen, J. Xiao, Q. Liu, and Z. Zhou, “Complex eigenvalue analysis of railway curve squeal,” in *Noise and Vibration Mitigation for Rail Transportation Systems*, pp. 433–439, Springer, 2008.